Quantum ergodicity of a coherence-preserving SU(2) Hamiltonian system with quasiperiodic kicking

Christopher C. Gerry and Thomas Schneider
Department of Physics, Saint Bonaventure University, Saint Bonaventure, New York 14778
(Received 13 April 1989)

In this paper we study the time evolution of a quasiperiodically kicked spin system whose Hamiltonian is linear in the SU(2) generators. Since this Hamiltonian preserves SU(2) coherent states under time evolution, there is a close correspondence between the quantum evolution and the classical evolution of the system on the Bloch sphere. Such a system has previously been studied by Milonni, Ackerhalt, and Goggin [Phys. Rev. A **35**, 1714 (1987)] and, with two incommensurate driving frequencies, the quantum evolution was characterized by (a) decay of the autocorrelation function of the state vector, (b) broadband power spectrum of observables, (c) ergodicity on the Bloch sphere. We expand upon their work to study the corresponding behavior of the motion on a symplectic phase space and the decay of the autocorrelation function of the state vector. When the forcing strength is such that the motion is localized in phase space, the autocorrelation function shows revivals. When the motion is ergodic the autocorrelation function rapidly decays without revivals. The classical motion however is not chaotic, there is no sensitive dependence on initial conditions. For three incommensurate frequencies, the motion is more delocalized than for two frequencies for a fixed forcing strength.

I. INTRODUCTION

There is currently considerable interest in the fundamental question of how quantum mechanics can exhibit the phenomenon of what is now called "chaos".[1] It is in fact debatable as to whether or not the notion of quantum chaos, unlike classical chaos, has any meaning.[2] Early numerical experiments by Casati *et al.*[3] found that for a periodically kicked rotor, quantum effects greatly suppress the diffusive energy growth associated with the classical time evolution of the model given by the so-called standard map. A general theorem has been proved[4] that shows that for time-periodic Hamiltonian systems that are nonresonant and bounded, the system will reassemble itself infinitely often in time. For the kicked rotor, the resultant quantum suppression of chaos can be related to the problem of Anderson localization of a particle on a one-dimensional lattice with a random potential.[5]

With no real consensus on how to define quantum chaos, it is not surprising to find a great variety of definitions in the literature.[6] Also one ought to distinguish between time-independent and time-dependent systems, where progress in the former case has been made.[7] Generally speaking it seems that the term "quantum chaos" has come to mean the quantum behavior of any system whose classical counterpart is chaotic. However, recently there has been an attempt to characterize quantum chaos for driven quantum systems where the driving force need not be periodic but may be quasiperiodic instead. Pomeau *et al.*[8] have considered the quantum chaos of a two-level system with a time-dependent perturbation. When the perturbation is quasiperiodic with two incommunsurate frequencies, quantum chaos is present if the definition is taken to be a rapidly decaying autocorrelation function of the state vector and a broadband power spectrum for time-dependent observables (e.g., the inversion associated with the Rabi oscillations). However, it was lamented that the most important characterization of chaos, positive Lyapunov characteristic exponents (LCE's), are not possible in view of the conservation of the norm of the state vector. More recently, Milonni *et al.*[9] considered a quasiperiodically kicked two-level system, but added to the criterion of quantum chaos the fact that the motion on the Bloch sphere appears ergodic for strong quasiperiodic kicking. They did point out, however, that memory of the initial state is retained. They also applied quasiperiodic kicking to the rotor problem and confirmed the result of Shepelyansky,[10] that the Anderson localization effect is greatly weakened.

In the present work we wish to examine once again the quasiperiodically kicked two-level system. The main motivation for the current study is to make a clearer connection between the behavior of the autocorrelation function of the state vector and the type of motion we find in the associated classical phase space. We actually consider a slightly more general problem than in Ref. 9 where we take a Hamiltonian which is a linear combination of the generators of SU(2) and where the initial state is a generalized coherent state associated with the group.[11] For the irreducible representation where $j=\frac{1}{2}$, this will be the two-level system of Ref. 9 but with the initial state being a coherent superposition of the two levels. Hamiltonians which are linear in the SU(2) generators will preserve SU(2) coherent states (CS's) under time evolution. In this sense, as for ordinary coherent states,[12] the quantum-mechanical motion is determined by the classical motion in phase space. For the SU(2) problem, the available phase space is in fact bounded on the Bloch sphere. In our study we shall use a complex-plane representation of phase space $q+ip$ where the boundary of the accessible phase space is a circle whose radius is determined by j. This provides a useful display of phase space for the classification of the types of motion that will arise. Our first application is to the quasiperiodic kicking with two incommensurate frequencies. We find that when the motion (for low forcing strength) is confined to a narrow circular region of phase space, the autocorrelation function of the state vector (as well as for position coordinate q) shows periodic revivals. Also the power spectrum of q shows only discrete frequencies. As the strength of the pulsing is increased the motion eventually fills up the available phase space, the autocorrelation functions of the state vector and coordinate q rapidly decay, and the power spectrum of q becomes broadband. In this sense, the classical motion is essentially ergodic. However it is not chaotic as the LCE for the classical motion can be determined to be less than zero. In fact, we have graphically checked that nearby initial conditions give orbits that stay nearby. Thus, we do not have underlying classical chaos in this model so that the decay of the autocorrelation function and the broadbandedness of the power spectra seem to be associated with ergodicity only. The important point is that in our model, the quantum and classical motions closely correspond because of the coherence-preserving property of the Hamiltonian. This is unlike the study of the kicked top,[13] where the Hamiltonian is not coherence preserving. The second feature of our work is that we extend the calculations to the case of three incommensurate frequencies. As expected, this has the effect of causing greater delocalization of the motion in phase space for a given forcing strength. Ergodicity initially occurs for lower strength.

This paper is organized as follows. In Sec. II we present the general formalism of the model and, using group-theoretical methods, determine the motion for an initial SU(2) coherent state. A similar method has already been used to study pulsed SU(1,1) coherent states.[14] In Sec. III we present our results for the case $j=\frac{1}{2}$ for two and three incommensurate frequencies. Section IV contains some brief remarks and a summary.

II. THE MODELS

The Lie algebra of SU(2) is given by the commutation relations of the Su(2) generators J_0 and $J_\pm$ as

$$[J_0,J_\pm]=\pm J_\pm,\quad [J_-,J_+]=-2J_0 \tag{2.1}$$

and $J^2=J_0^2+J_1^2+J_2^2$ is the Casimir operator. The representation-space vectors $|j,m\rangle$ are eigenstates of J_0 and J^2 according to

$$J_0|jm\rangle=m|jm\rangle,\quad J^2|jm\rangle=j(j+1)|jm\rangle . \tag{2.2}$$

These basis states are of course complete with respect to m. SU(2) CS (Ref. 11) are formed from the representation space by the application of a displacement-type operator $D(\alpha)$ to the "ground" state $|j,-j\rangle$ of the representation where

$$D(\alpha)=\exp(\alpha J_+ -\alpha^* J_-) , \tag{2.3}$$

and $\alpha=-(\theta/2)e^{-i\phi}$. The angles θ and ϕ have the ranges $0\le\theta\le\pi$ and $0\le\phi\le 2\pi$ and parameterize the Bloch sphere.[15] With the above definition of α the SU(2) CS are given as[11]

$$\begin{aligned}|\zeta\rangle &= D(\alpha)|j,-j\rangle \\ &=(1+|\zeta|^2)^{-j} \\ &\quad\times\sum_{m=-j}^{j}\left[\frac{(2j)!}{(j+m)!(j-m)!}\right]^{1/2}\zeta^{j+m}|jm\rangle ,\end{aligned} \tag{2.4}$$

where $\zeta=-\tan(\theta/2)e^{-i\phi}$.

The parameter ζ may be interpreted as a complex number representing the classical phase space associated with the SU(2) CS of Eq. (2.4). Indeed, with the Hamiltonian H composed of the SU(2) generators, from the path-integral expression of the propagator calculated over the SU(2) CS,[16] one obtains in the classical limit, Hamilton's equations for ζ as

$$\dot\zeta=\{\zeta,\mathcal{H}\},\quad \dot\zeta^*=\{\zeta,\mathcal{H}\} , \tag{2.5}$$

where $\{A,B\}$ is the Poisson bracket given by

$$\begin{aligned}\{A,B\} &= i\frac{(1+|\zeta|^2)^2}{2j}\left[\frac{\partial A}{\partial\zeta^*}\frac{\partial B}{\partial\zeta}-\frac{\partial A}{\partial\zeta}\frac{\partial B}{\partial\zeta^*}\right] \\ &=\frac{1}{j\sin\theta}\left[\frac{\partial A}{\partial\phi}\frac{\partial B}{\partial\theta}-\frac{\partial A}{\partial\theta}\frac{\partial B}{\partial\phi}\right]\end{aligned} \tag{2.6}$$

and where $\mathcal{H}=\langle\zeta|H|\zeta\rangle$. The Poisson bracket above indicates the classical phase space is that of a sphere.[17] However, it is convenient to use an alternate form in parameterizing the phase space. We define the parameter[18]

$$\begin{aligned}z &= \frac{1}{\sqrt{2}}(q+ip)=(2j)^{1/2}\frac{\alpha}{|\alpha|}\sin(|\alpha|) \\ &=-(2j)^{1/2}e^{-i\phi}\sin\left[\frac{\theta}{2}\right] ,\end{aligned} \tag{2.7}$$

which has the effect of flattening the phase space in the sense that now we have the usual symplectic form of Hamilton's equations

$$\dot q=\frac{\partial\mathcal{H}}{\partial p},\quad \dot p=-\frac{\partial\mathcal{H}}{\partial q} . \tag{2.8}$$

The most general Hamiltonian which preserves an arbitrary SU(2) CS under time evolution has the form

$$H(t)=\Omega(t)J_0+f(t)J_+ + f^*(t)J_- +\beta(t) , \tag{2.9}$$

where $\Omega(t)$ is a real, and $f(t)$ is an imaginary, function of time, and $\beta(t)$ is an arbitrary real function of time. The proof of this follows along the same lines as for the SU(1,1) CS.[19] In this work, we follow Refs. 9 and 10 and take the forcing term to consist of a periodic sequence of δ functions modulated by a function of time $F(t)$ which itself may be periodic or quasiperiodic. Thus we take

$$f(t)=F(t)\sum_{n=-\infty}^{\infty}\delta(t-nT) , \tag{2.10}$$

where $T>0$ and is the period of the pulses. The frequency of the pulses is $\omega=2\pi/T$. With $\beta(t)=0$ *and* with $\Omega=2\omega_0=$const (the factor of 2 is for convenience) we have

$$H(t)=2\omega_0 J_0+2J_1 F(t)\sum_{n=-\infty}^{\infty}\delta(t-nT) , \quad (2.11)$$

where $J_1=(J_+ + J_-)/2$.

If the state vector prior to the nth δ-function pulse is designated as $|\psi(n)\rangle$, then just after the nth pulse the state vector is

$$|\psi(n)\rangle'=e^{-2iJ_1F(nT)}|\psi(n)\rangle . \quad (2.12)$$

Between the pulses, the free evolution is governed by the free Hamiltonian $H_0=2\omega_0 J_0$ so that just before the $(n+1)$th pulse, the state vector is

$$|\psi(n+1)\rangle=U(n)|\psi(n)\rangle , \quad (2.13)$$

where

$$U(n)=\exp(-2i\omega_0 TJ_0)\exp[-2iF(nT)J_1] . \quad (2.14)$$

In the $j=\frac{1}{2}$, 2×2 representation, the exponential operators in the above have the form

$$e^{-2i\omega_0 TJ_0}_{(2\times2)}=\begin{bmatrix} e^{-\omega_0 T} & 0 \\ 0 & e^{-i\omega_0 T}\end{bmatrix} , \quad (2.15)$$

$$e^{-2iF(nT)J_1}_{(2\times2)}=\begin{bmatrix} \cos[F(nT)] & -i\sin[F(nT)] \\ -i\sin[F(nT)] & \cos[F(nT)]\end{bmatrix} . \quad (2.16)$$

Thus in the 2×2 representation, the evolution operator $U(n)$ corresponds to the group transformation

$$U(n)_{(2\times2)}=\begin{bmatrix} a_n & b_n \\ -b_n^* & a_n^*\end{bmatrix},\quad |a_n|^2+|b_n|^2=1 \quad (2.17)$$

where

$$a_n=e^{-i\omega_0 T}\cos[F(nT)] ,$$
$$b_n=-ie^{-i\omega_0 T}\sin[F(nT)] . \quad (2.18)$$

We now assume that the initial state at $n=0$ is an SU(2) CS which we denote as $|\zeta_0,0\rangle\equiv|\zeta_0\rangle$. The evolution operator acts to produce

$$|\zeta_0,1\rangle=U(0)|\zeta_0,0\rangle ,$$
$$\vdots \quad (2.19)$$
$$|\zeta_0,i+1\rangle=U(i)|\zeta_0,i\rangle .$$

However, the action of a finite group transformation $T^{(j)}(g)$, where

$$g=\begin{bmatrix} a & b \\ -b^* & a^*\end{bmatrix},\quad |a|^2+|b|^2=1 \quad (2.20)$$

on an SU(2) CS $|\zeta\rangle$ is given as

$$T^{(j)}(g)|\zeta\rangle=e^{i\Phi}|\zeta'\rangle , \quad (2.21)$$

where

$$\zeta'=\frac{a\zeta+b}{a^*-b^*\zeta},\quad \Phi=2j\arg(a^*-b^*\zeta) \quad (2.22)$$

(see Appendix). Thus we have

$$|\zeta_0,1\rangle=U(0)|\zeta_0,0\rangle=e^{i\Phi_0}|\zeta_1\rangle ,$$
$$|\zeta_0,2\rangle=U(1)|\zeta_0,1\rangle=e^{i(\Phi_0+\Phi_1)}|\zeta_2\rangle ,$$
$$\vdots \quad (2.23)$$
$$|\zeta_0,n+1\rangle=U(n)|\zeta_0,n\rangle=e^{i(\Phi_0+\Phi_1+\cdots+\Phi_n)}|\zeta_{n+1}\rangle ,$$

where

$$\zeta_{n+1}=\frac{a_n\zeta_n+b_n}{a_n^*-b_n^*\zeta_n},\quad \Phi_n=2j\arg(a_n^*-b_n^*\zeta_n) . \quad (2.24)$$

These equations define the Poincare maps in the complex plane which have the form of Mobius transformations.[20] However, the ζ plane is also the equatorial plane of the Bloch sphere since $\zeta=-\tan(\theta/2)e^{-i\phi}$ actually performs a stereographic projection from the Bloch sphere onto the equatorial plane.[21] By inverting ζ_n, the Poincaré map can be projected on the symplectic phase space from Eq. (2.7) as

$$q_n=-2\sqrt{j}\,\sin\left[\frac{\theta_n}{2}\right]\cos(\phi_n) ,$$
$$p_n=2\sqrt{j}\,\sin\left[\frac{\theta_n}{2}\right]\sin(\phi_n) . \quad (2.25)$$

Between pulses the expectation values of observables may be calculated using the $|\zeta_0,n\rangle$. For example, the energy just before the nth pulse is

$$E_n=\langle\zeta_0,n|H_0|\zeta_0,n\rangle=-2j\omega_0\left[\frac{1-|\zeta_n|^2}{1+|\zeta_n|^2}\right] . \quad (2.26)$$

Finally in this section, we derive the autocorrelation function (ACF) of the state vector, defined as[8]

$$C(\tau)=\lim_{T\to\infty}\frac{1}{T}\int_0^T\langle\psi(t)|\psi(t+\tau)\rangle dt . \quad (2.27)$$

For our pulsed system this may be written in the discretized form[9]

$$C(l)=\lim_{N\to\infty}\frac{1}{N}\sum_{n=0}^{N}\langle\zeta_0,n|\zeta_0,n+l\rangle . \quad (2.28)$$

[Note that this is normalized such that $C(0)=1$.] Using Eqs. (2.22) we have

$$C(l)=\lim_{n\to\infty}\frac{1}{N}\sum_{n=0}^{N}e^{i(\Phi_n+\cdots+\Phi_{n+l})}\langle\zeta_n|\zeta_{n+l}\rangle . \quad (2.29)$$

The inner product in Eqs.(2.8) can be calculated in closed form as[11]

$$\langle\zeta_n|\zeta_{n+1}\rangle=\frac{(1+\zeta_n^*\zeta_{n+l})^{2j}}{(1+|\zeta_n|^2)^j(1+|\zeta_{n+l}|^2)^j} . \quad (2.30)$$

III. APPLICATIONS

A. Quasiperiodic forcing with two incommensurate frequencies

We first consider the case studied by Milonni *et al.*[9] where $F(t)$ has the form $F(t)=\lambda\cos(\omega' t)$. Thus we have $F(nT)=\lambda\cos(2\pi\chi n)$, where $\chi=\omega'/\omega$. We shall only consider the case when ω' and ω are incommensurate and hence χ is irrational. This is approximated by writing ω' and ω as the ratios of large prime numbers. We follow Refs. 8, 9, and 11 and write $\chi=\frac{4637}{13\,313}$, which is "irrational" for practical purposes. We set $\omega_0 T=0.126$ and we

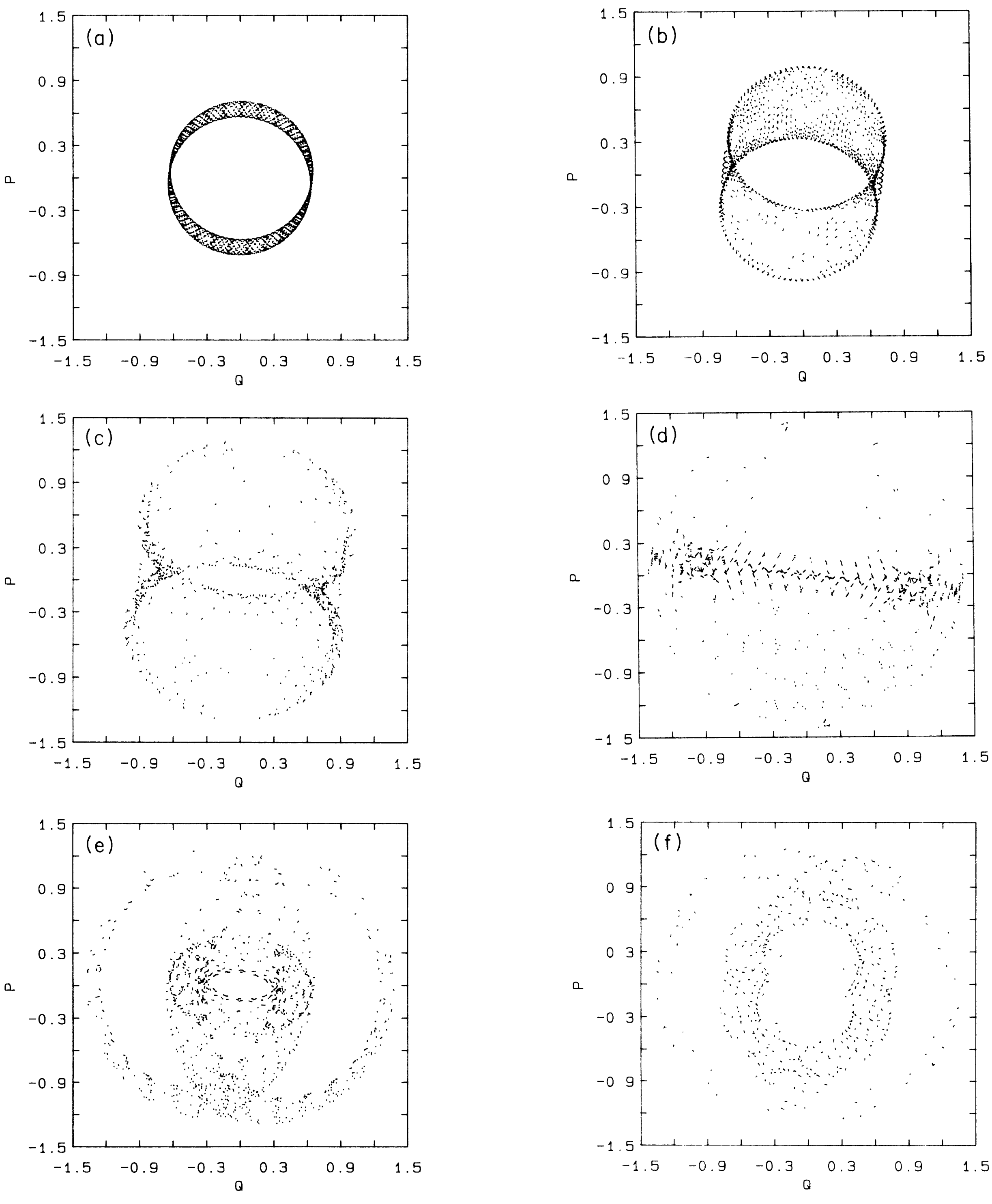

FIG. 1. Poincaré plots for two incommensurate frequencies. (a) $\lambda=0.1$, (b) $\lambda=0.5$, (c) $\lambda=1.00$, (d) $\lambda=1.46$, (e) $\lambda=3.00$, (f) $\lambda=3.50$, (g) $\lambda=4.00$, (h) $\lambda=5.00$, (i) $\lambda=500$.

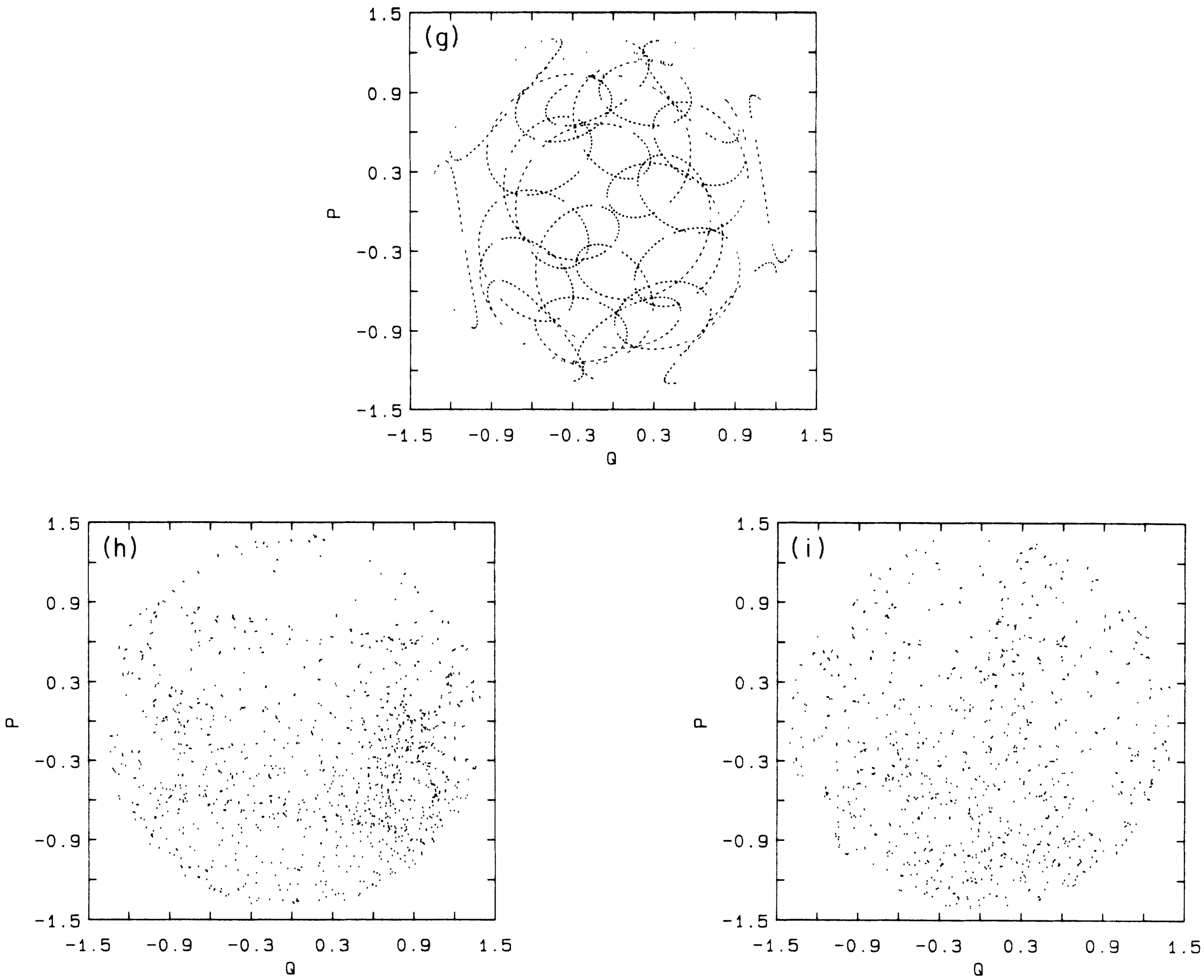

FIG. 1. (*Continued*).

take $\zeta_0=0.5$. Only the case of $j=\frac{1}{2}$ is considered.

In Fig. 1 we display the iterated Poincaré maps in the $p-q$ phase space for increasing λ. 2500 points are plotted. In Fig. 2 we display the corresponding ACF's of the state vector. In Fig. 3 we display the power spectrum of the classical variable q.

As λ increases it is apparent that the motion in the space becomes less localized. For the case of small λ as in Figs. 1(a)–1(c) where $\lambda=0.1$, 0.5, and 1.0, respectively, the motion appears to be quite regular with the basic $\lambda=0$ circle slowly oscillating back and forth. That the motion for low λ appears quite regular and periodic can be readily explained. With $F(nT)=\lambda\cos(2\pi\chi n)$, from Eq. (2.18) we have

$$a_n=e^{-i\omega_0 T}\cos[\lambda\cos(2\pi\chi n)]\ ,$$
$$b_n=-ie^{-i\omega_0 T}\sin[\lambda\cos(2\pi\chi n)]\ . \tag{3.1}$$

The function $\cos[\lambda\cos(2\pi\chi n)]$ and $\sin[\lambda\cos(2\pi\chi n)]$, as was shown in Ref. 9, for large λ and irrational χ are themselves "chaotic" in the sense that the functions vary erratically and their autocorrelation functions exhibit rapid decay. However for very small λ, we may approximate a_n and b_n as

$$a_n\approx e^{-i\omega_0 T}\ ,$$
$$b_n\approx -i\lambda e^{-i\omega_0 T}\cos(2\pi\chi n)\ , \tag{3.2}$$

where only terms up to order λ have been retained. Under this approximation the mapping is clearly periodic. For somewhat larger λ, more terms must be retained in the expansions of $\sin[\lambda\cos(2\pi\chi n)]$ and $\cos[\lambda\cos(2\pi\chi n)]$. The coefficients then become quasiperiodic, the motion becoming more irregular as more frequencies contribute to the motion. For instance, retaining terms up to order λ^2 we obtain

$$a_n\approx e^{-i\omega_0 T}\left[1-\frac{\lambda^2}{4}[1+\cos(4\pi\chi n)]\right]\ ,$$
$$b_n\approx -i\lambda e^{-i\omega_0 T}\cos(2\pi\chi n)\ , \tag{3.3}$$

which involves two frequencies that are simple multiples.

For the small values of $\lambda=0.1$, 0.5, and 1.0 the motion is quite localized in phase space. The fact that the motion in the occupied regions is regular is apparent

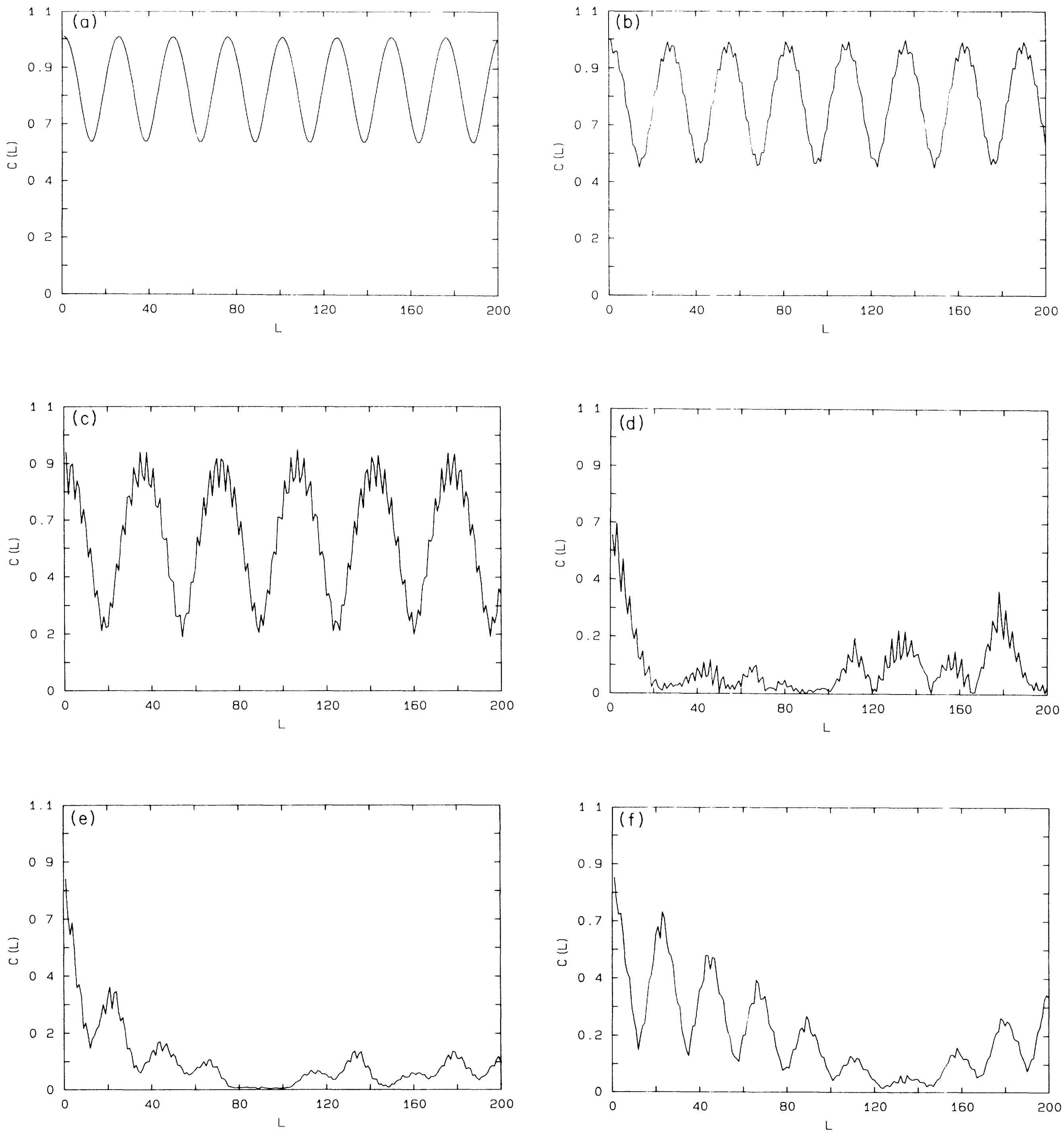

FIG. 2. Autocorrelation junction for the state vector for the same sequence of λs as in Fig. 1.

from the corresponding ACF (Fig. 2) where the oscillations are regular and the power spectrum of q (Fig. 3) shows contributions from only a few frequencies. As λ is increased, the motion occupies more volume in phase space, the ACF shows still some regularity, and the power spectrum shows more spikes. At $\lambda=1.46$, the motion expands out to the radius $2\sqrt{j}$ of the allowed phase space. Nevertheless, there is still some regular behavior here as is clear from Fig. 1(d) and the fact that the ACF does revive somewhat after the initial decay. Increasing to $\lambda=3.00$, we find quite surprisingly that the motion appears to be more localized in phase space than in the previous case. The power spectrum shows fewer frequencies in this case as well and the ACF shows a slower decay initially. At $\lambda=3.50$ the ACF decays even slower. At $\lambda=4.00$ the motion appears like a sufrace of section of a perfectly regular, but complicated, torus. It is interesting that the plotted points do not represent a

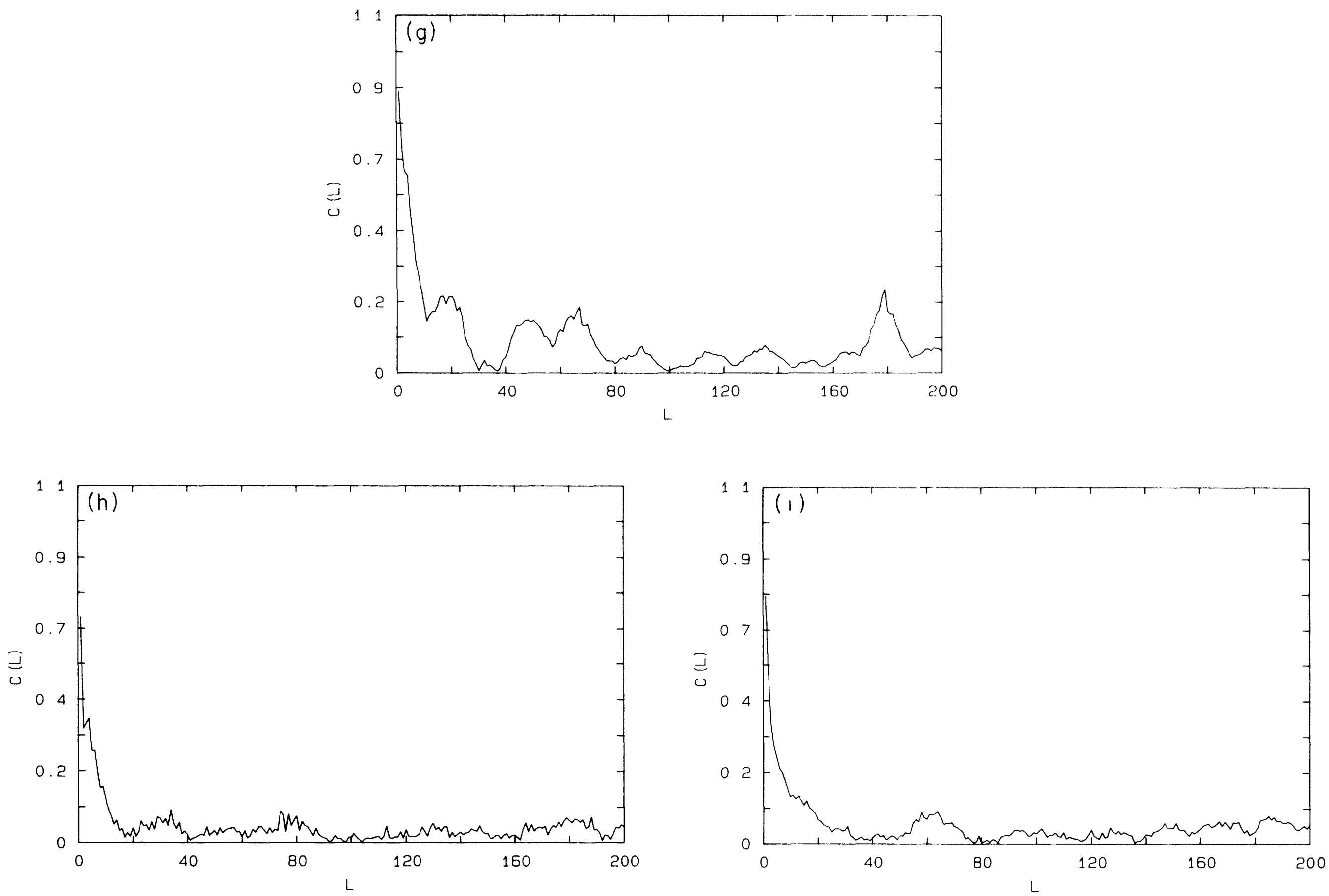

FIG. 2. (*Continued*).

continuous trajectory, i.e., nearby points are not necessarily sequential. In watching the pattern build up, the points seem to appear randomly in time. At $\lambda=5.00$, the motion once again fulls up the allowed phase space but nevertheless, there appears within the noise, a boxlike region with straight caustics. Finally with $\lambda=500$, we have phase space filled up uniformly and we conclude that the motion is essentially ergodic. Also in this case the ACF drops down much faster and lower and does not exhibit significant revivals. Also the power spectrum in this case is very broadband.

In spite of the behavior observed in the case of $\lambda=500$, there is really no true chaos involved. We have followed the motion of two initially nearby points in phase space and found that they remain nearby for increasing n. We have corroborated this observation with a calculation of the LCE which is always negative and approaches zero as $\lambda\rightarrow\infty$.

B. Three incommensurate frequencies

We now take $F(t)$ to be of the form

$$F(t)=\lambda\cos(\omega' t)\cos(\omega'' t)\ . \qquad (3.4)$$

Then we have

$$F(nT)=\lambda\cos(2\pi\chi_1 n)\cos(2\pi\chi_2 n)\ , \qquad (3.5)$$

where $\chi_1=\omega'/\omega$ and $\chi_2=\omega''/\omega$. We take $\chi_1=\frac{4637}{13\,313}$ and $\chi_2=\frac{2197}{7253}$ to approximate three incommensurate frequencies.

In Fig. 4 we display the phase space motion for various λ. In Fig. 5 we have the corresponding autocorrelation functions of the state vector and in Fig. 6, the corresponding power spectra for the variable q.

In this case it appears that the effect of the third incommensurate frequency, for a given λ, is to further delocalize the motion in phase space. For low λ, some interesting patterns arise. As λ increases more area of phase space is occupied by the motion (except for certain values of λ). At $\lambda=1.4$ the motion appears to be essentially ergodic. The reason for the more delocalized motion is clear since even at low λ, from the previous analysis in Sec. III A, the coefficients a_n and b_n will depend on two incommensurate frequencies.

C. Correlation function of the coordinate q

So far we have discussed the autocorrelation function of the state vector and the power spectrum of the coordinate q. We have observed that the power spectrum becomes broadband for increasing λ. Here we would like to

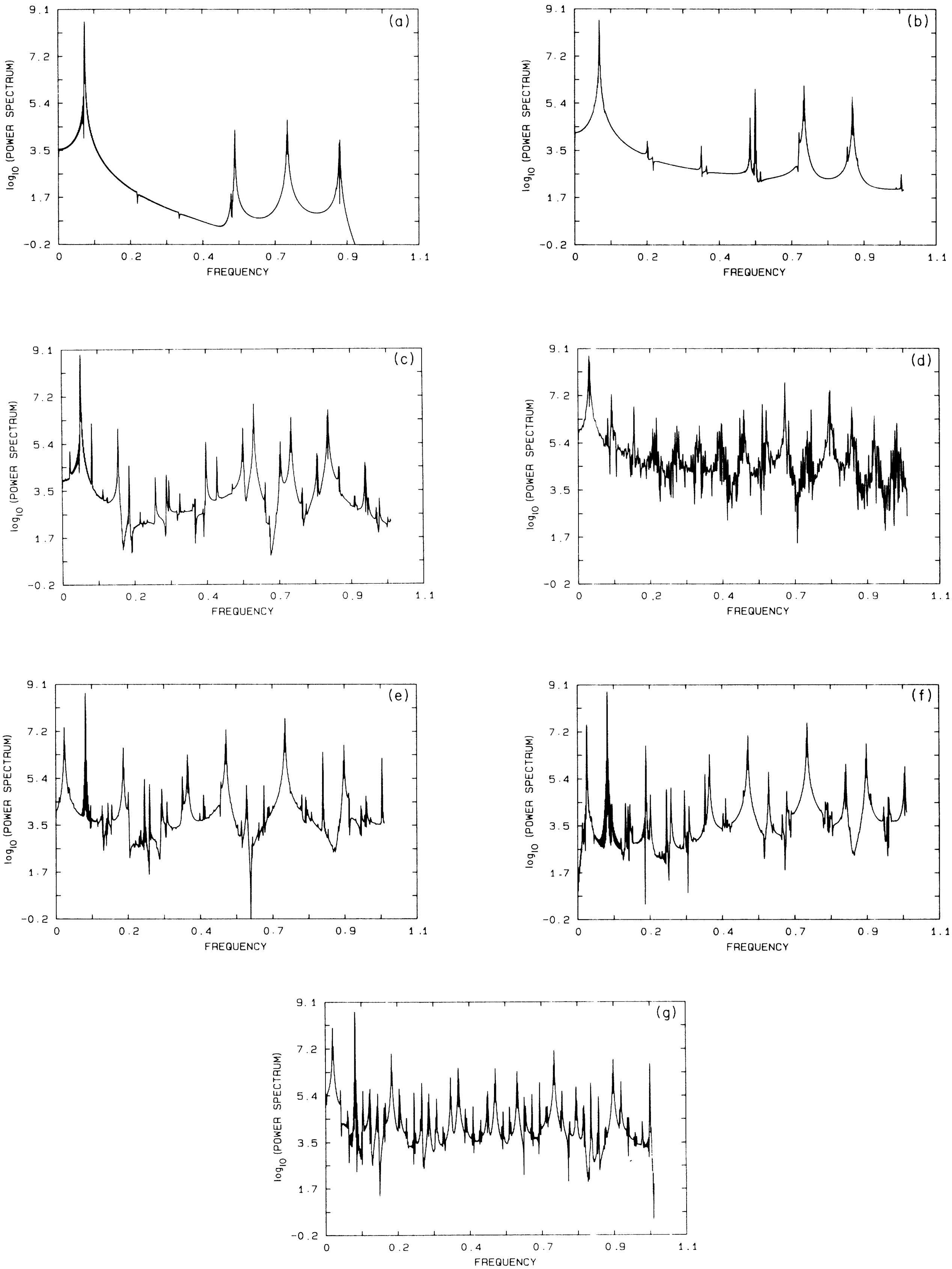

FIG. 3. Power spectrum of q for the same sequence of λs as Fig. 1.

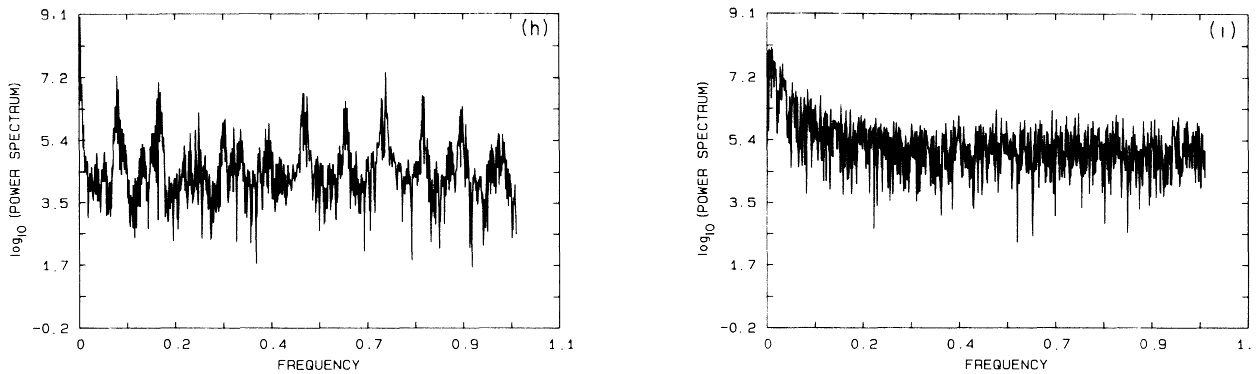

FIG. 3. (*Continued*).

point out that the decay of the autocorrelation function of the state vector is not necessarily associated with similar behavior in the autocorrelation function of q, which is defined as[22]

$$C_q(l)=\lim_{N\to\infty}\frac{1}{N}\sum_n q_n q_{n+l}-\bar{q}^{\,2}\ , \tag{3.6}$$

where

$$\bar{q}=\lim_{N\to\infty}\frac{1}{N}\sum_{n=0}^{\infty} q_n\ . \tag{3.7}$$

For example, in the two-frequency case with $\lambda=4.00$, $C_q(l)$ shows many revivals [see Fig. 7(a)] in contrast to

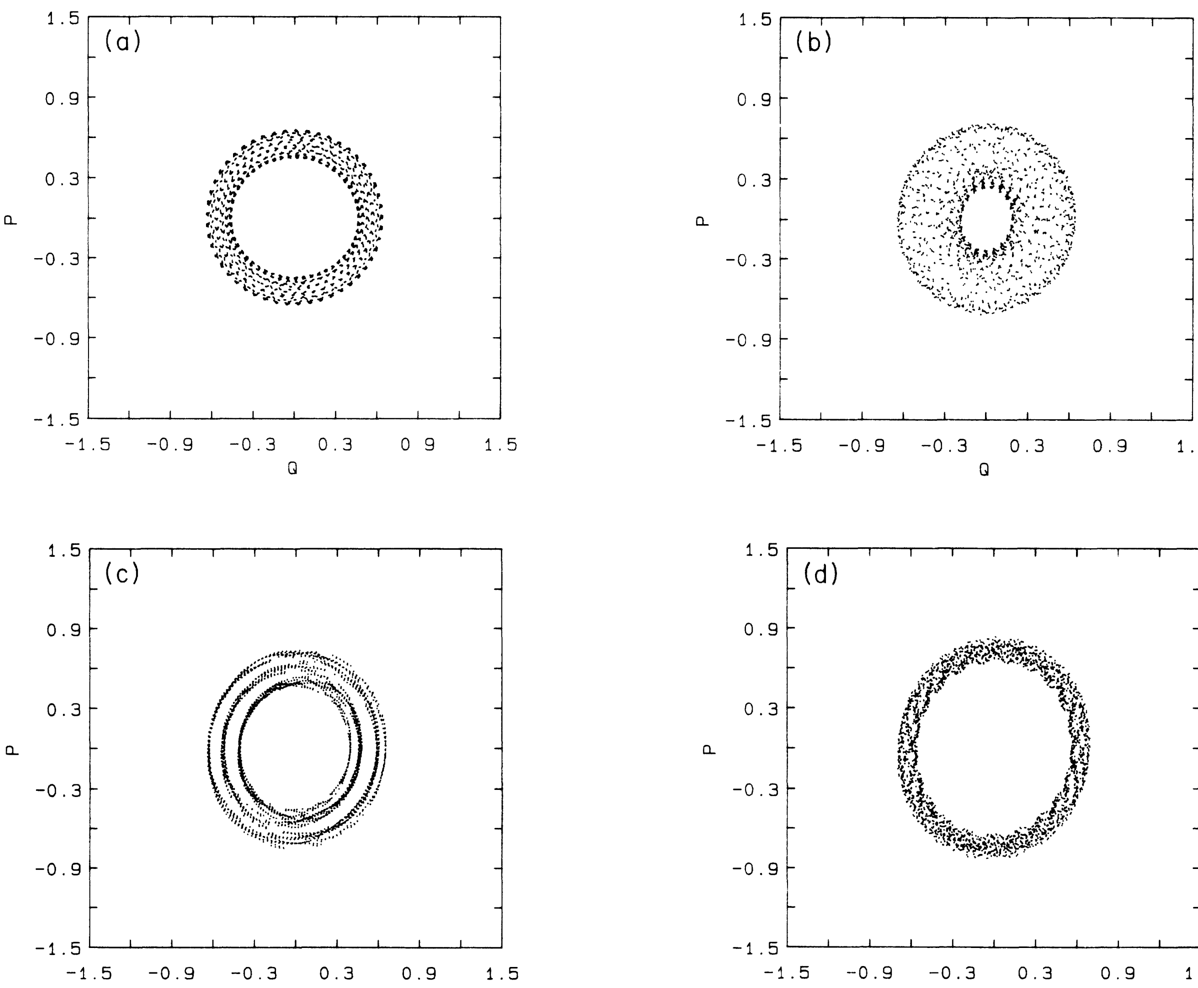

FIG. 4. Poincaré plots for three incommensurate frequencies. (a) $\lambda=0.01$, (b) $\lambda=0.05$, (c) $\lambda=0.07$, (d) $\lambda=0.1$, (e) $\lambda=0.5$, (f) $\lambda=1.4$, (g) $\lambda=4.0$.

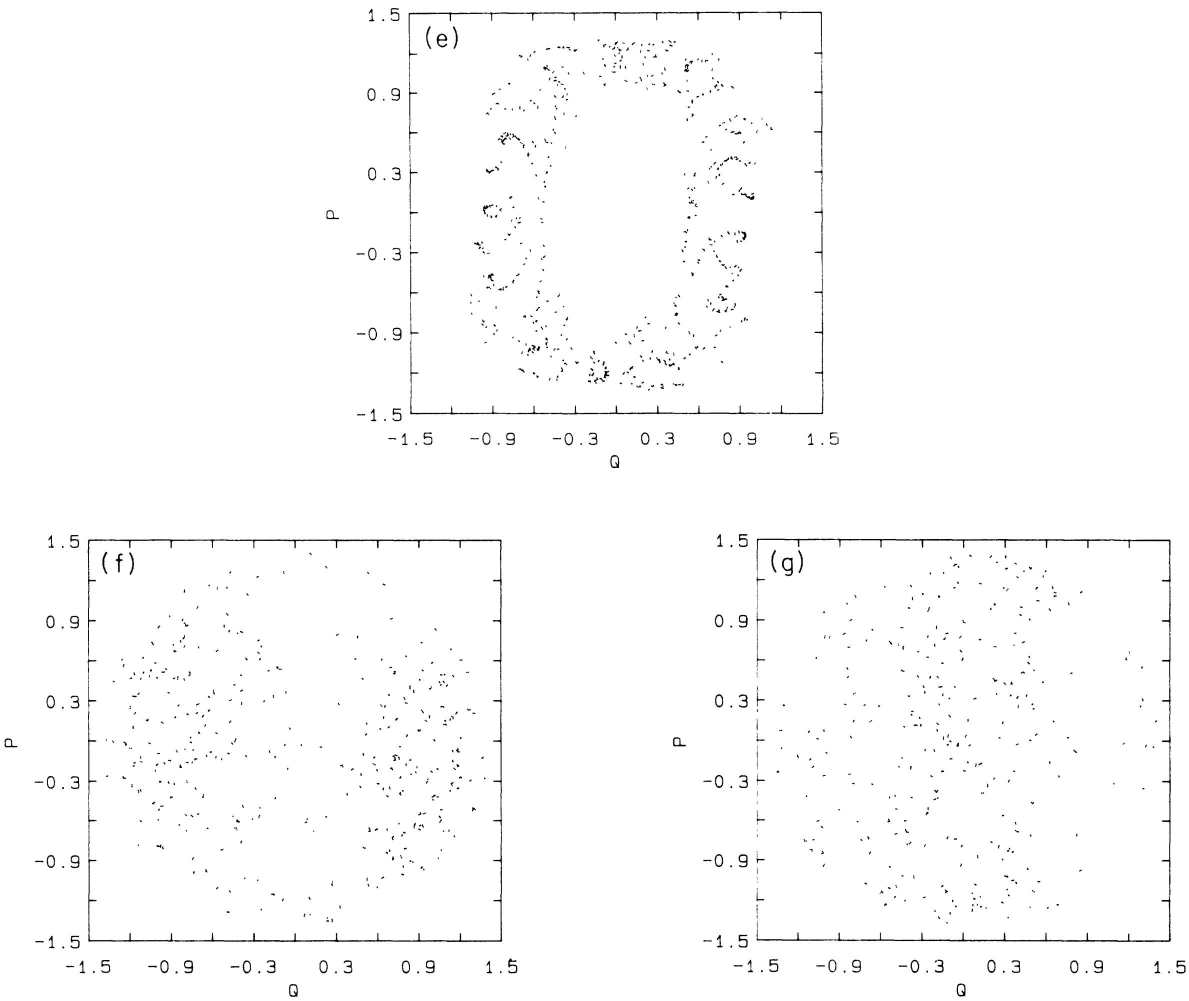

FIG. 4. (*Continued*).

the behavior of the autocorrelation function of the state $C(l)$. This, of course, is reflected in the many discrete spikes in the power spectrum. For $\lambda=500$, $C_q(l)$ is very low for most of the time [Fig. 7(b)]. In the three-frequency case, for $\lambda=1.4$, again we see revivals in $C_q(l)$ not exhibited by $C(l)$ [Fig. 7(c)]. At $\lambda=4.00$, $C_q(l)$ again drops rapidly as does $C(l)$.

IV. DISCUSSION

In most discussions of quantum chaos, the classical counterpart of the system under study exhibits chaotic behavior. In this study we have considered a model where the quantum evolution is determined by the classical evolution. Using quasiperiodic perturbations, the motion has been shown to be localized in phase space for certain strengths λ but more delocalized, generally, as λ is increased, eventually becoming essentially ergodic. Increasing the number of incommensurate frequencies causes more delocalization for a given λ. The motion is never chaotic, however, since the $\overline{\mathrm{LCE}}$ is always negative. Thus, the decay of the autocorrelation function of the state vector, which has previously been used in one definition of "quantum chaos",[8,9] might best be referred to as the criterion for "quantum ergodicity," a much weaker kind of randomness. It is important to note, however, that even this must be qualified in view of the remarks of Sec. III C. Nevertheless for very high λ, both $C(l)$ and $C_q(l)$ decay very rapidly and the power spectrum of q is broadband. This should be considered as an indication of the corresponding classical-quantum ergodicity. Since the decay of the ACF of the state vector has previously been taken as a signal for quantum chaos,[23] it would be interesting to see if this decay is more properly associated with only the weaker conditions of ergodicity in models which do not preserve coherent states.

Finally let us mention the role of j in our calculations. As is well known, the limit $j\rightarrow\infty$ is considered to be a classical limit. However, in the present calculation, the quantum phase-space map that we obtain, Eq. (2.24), is independent of j. This is because the driving Hamiltoni-

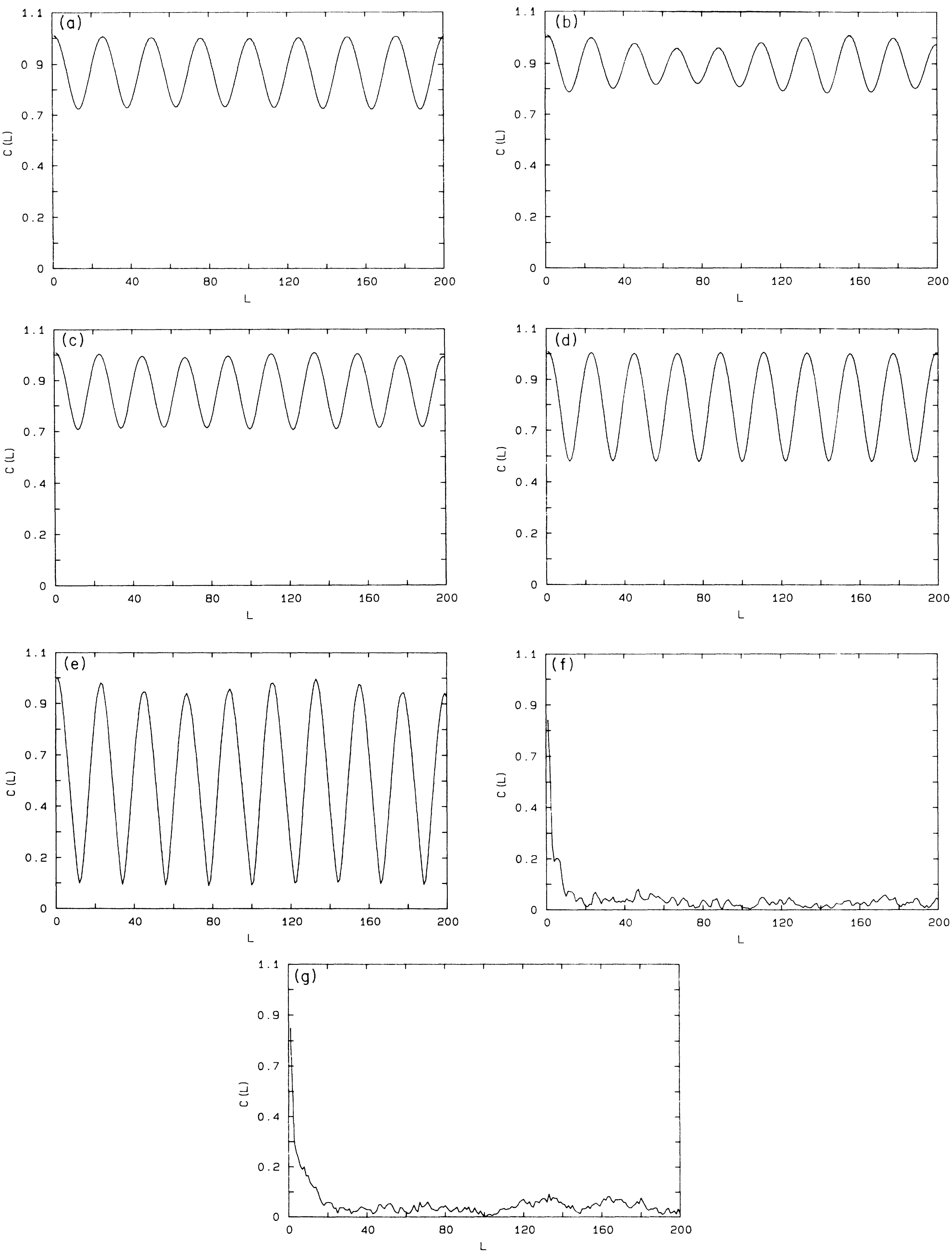

FIG. 5. Autocorrelation function of the state vector for the same sequence of λs as in Fig. 4.

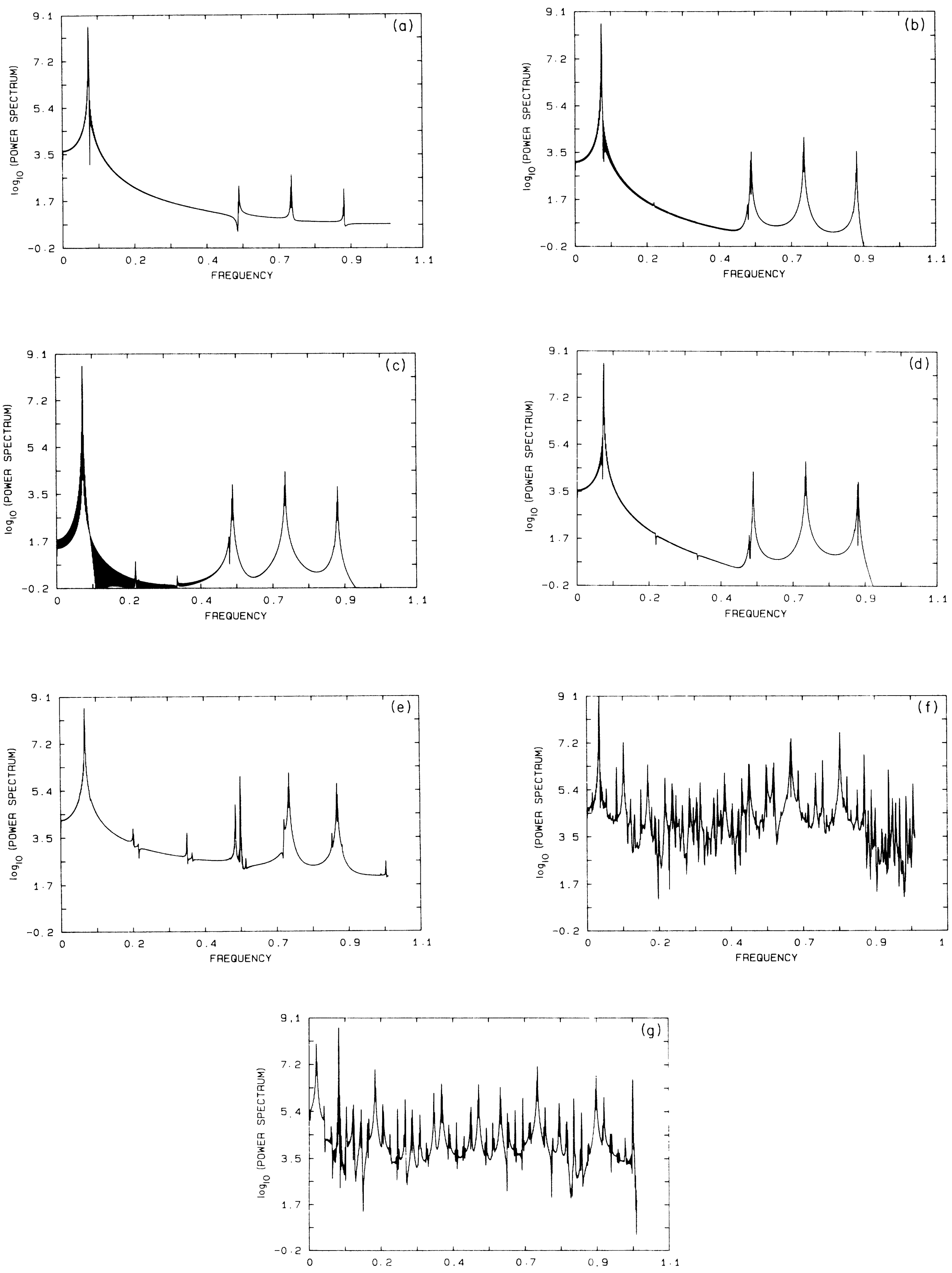

FIG. 6. Power spectrum of q for the same sequence of λs as in Fig. 4.

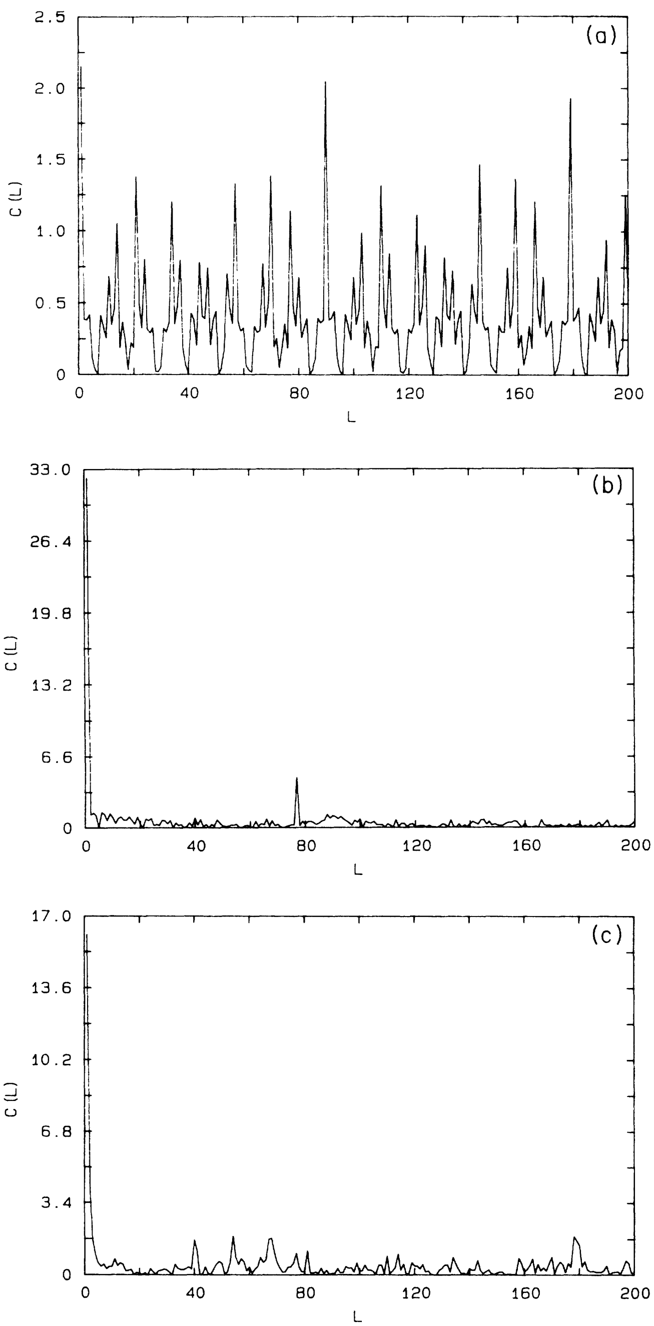

FIG. 7. Autocorrelation function of q in the two-frequency case with (a) $\lambda=4.00$, (b) $\lambda=5.00$ and in the three frequency case (c) with $\lambda=4.00$.

an is linear in the generators of SU(2) thus preserving the coherence of an arbitrary initial SU(2) CS. The point of this is that the quantum and classical motions are the same even for finite j. The only effect j has is to define the size of the phase space as a scale factor in Eq. (2.25) and it appears in the autocorrelation function (2.29). We have tried other j values and have found no essential change in the ACF. Of course, for models which do not preserve SU(2) CS, such as the one studied in Ref. 13, one does expect to find differences in the quantum and classical motion. It has been possible to show a distinction between regular and irregular behavior for times exceeding a certain quantum-mechanical quasiperiod where classical behavior (chaotic or regular) has died out by quantum means. However, as we have said in the model studied, there is no essential distinction between the quantum and classical evolutions.

ACKNOWLEDGMENTS

One of us (C.C.G.) wish to thank Dr. Edward Vrscay for the clarification of some concepts related to this work.

APPENDIX

In this Appendix we derive the formulas of Eqs. (2.20) and (2.21).

Using the 2×2 realization of the SU(2) Lie algebra, the displacement operator $D(\alpha)=\exp(\alpha J_+ - \alpha^* J_-)$ with $\alpha=-(\theta/2)e^{-i\phi}$ can be shown to be

$$D(\alpha)_{(2\times2)}=\begin{bmatrix} \cos\left[\frac{\theta}{2}\right] & -e^{-\phi}\sin\left[\frac{\theta}{2}\right] \\ e^{i\phi}\sin\left[\frac{\theta}{2}\right] & \cos\left[\frac{\theta}{2}\right] \end{bmatrix} . \tag{A1}$$

Also, using the 2×2 realization, the operator $D(\alpha)$ can be written as

$$D(\alpha)_{(2\times2)}=e^{\zeta J_+}e^{\beta J_0}e^{-\zeta^* J_-}$$
$$=\begin{bmatrix} e^{\beta/2}-|\zeta|^2e^{-\beta/2} & \zeta e^{-\beta/2} \\ -\zeta^* e^{-\beta/2} & e^{-\beta/2} \end{bmatrix} . \tag{A2}$$

By comparing Eqs. (A1) and (A2) we have $\zeta=-\tan(\theta/2)e^{-i\phi}$ and $\beta=\ln(1+|\zeta|^2)$. Now if we consider the further operation of a finite group transformation $T^{(j)}(g)$ on $D(\alpha)$, where

$$T^{(j)}(g)_{(2\times2)}=\begin{bmatrix} a & b \\ -b^* & a^* \end{bmatrix} , \tag{A3}$$

then we have

$$T^{(j)}(g)D(\alpha)_{(2\times2)}=\begin{bmatrix} a\cos\frac{\theta}{2}-be^{i\phi}\sin\frac{\theta}{2} & ae^{-i\phi}\sin\frac{\theta}{2}+b\cos\frac{\theta}{2} \\ -b^*\cos\frac{\theta}{2}-a^*e^{-i\phi}\sin\frac{\theta}{2} & -b^*e^{-i\phi}\sin\frac{\theta}{2}+a^*\cos\frac{\theta}{2} \end{bmatrix} . \tag{A4}$$

We assume that the operator $T^{(j)}(g)D(\alpha)$ may also be expressed in the form $\exp(\zeta' J_+)\exp(\beta' J_0)\exp(-\zeta'^* J_-)$ whose 2×2 representation is as in Eq. (A2) with $\zeta\to\zeta'$ and $\beta\to\beta'$. By comparing terms again with Eq. (A4), we obtain (after some algebra)

$$\zeta' = \frac{a\zeta+b}{a^*-b^*\zeta} , \qquad \beta' = \ln(1+|\zeta'|^2) - 2i \arg(a^*-b^*\zeta) . \tag{A5}$$

Thus upon application to the ground state $|j,-j\rangle$, we obtain

$$T^{(j)}(g)D(\alpha)|j,-j\rangle = T^{(j)}(g)|\zeta\rangle = e^{i\Phi}|\zeta'\rangle , \tag{A6}$$

where

$$\Phi = 2j \arg(a^*-b^*\zeta) . \tag{A7}$$

[1]See, for example, Science **243**, 893 (1989).

[2]See *Chaotic Behavior in Quantum Systems,* Vol. 120 of *NATO Advanced Studies Institute, Series B: Physics,* edited by G. Casati (Plenum, New York, 1985).

[3]G. Casati, B. V. Chirikov, J. Ford, and F. M. Izrailev, *Stochastic Behavior in Classical and Quantum Systems,* Vol. 93 of *Lecture Notes in Physics,* edited by G. Casati and J. Ford (Springer, Berlin, 1979).

[4]T. Hogg and B. A. Huberman, Phys. Rev. A **28**, 22 (1983).

[5]D. R. Grempel and R. E. Prange, Phys. Rev. A **29**, 1639 (1984).

[6]See E. B. Stechl and E. J. Heller, Ann. Rev. Phys. Chem. **35**, 563 (1984); P. Pechukas, J. Chem. Phys. **88**, 4823 (1984).

[7]See S. Fishman, D. R. Grempel, and R. E. Prange, Phys. Rev. Lett. **49**, 509, 833 (1982); G. Casati and I. Guarneri, Commun. Math. Phys. **95**, 121 (1984); M. Berry, Physica (Amsterdam) **10D**, 369 (1984).

[8]Y. Pomeau, B. Dorizzi, and B. Grammaticos, Phys. Rev. Lett. **56**, 681 (1986).

[9]P. W. Milonni, J. R. Ackerhalt, and M. E. Goggin, Phys. Rev. A **35**, 1714 (1987).

[10]D. L. Shepelyansky, Physics D **8**, 208 (1983).

[11]A. Perelomov, *Generalized Coherent States and Their Applications* (Springer, Berlin, 1986).

[12]R. J. Glauber, Phys. Lett. **21**, 650 (1966).

[13]F. Haake, M. Kuś, and R. Scharf, Ziet. Phys. B **65**, 381 (1987).

[14]C. C. Gerry and E. R. Vrscay, Phys. Rev. A **39**, 5717 (1989).

[15]F. T. Arecchi, E. Courtens, R. Gilmore, and H. Thomas, Phys. Rev. A **6**, 2211 (1972).

[16]H. Kuratsuji and T. Suzuki, J. Math. Phys. **21**, 472 (1980).

[17]F. A. Berezin, Commun. Math. Phys. **40**, 153 (1975).

[18]W. M. Zhang, C. C. Martens, D. H. Feng, and J. M. Yuan, Phys. Rev. Lett. **61**, 2167 (1988).

[19]C. C. Gerry, Phys. Rev. A **31**, 2721 (1985).

[20]R. L. Devaney, *An Introduction to Chaotic Dynamical Systems* (Addison-Wesley, Reading MA, 1987), Chap. 3.

[21]See P. K. Aravind, J. Opt. Soc. Am. B **5**, 1545 (1988).

[22]See P. W. Milonni, M.-L. Shih, and J. R. Ackerhalt, *Chaos in Laser-Matter Interactions* (World Scientific, Singapore, 1987), p. 32.

[23]M. J. Davis, J. Phys. Chem. **92**, 3124 (1988).